Time-Dependent Boundary Conditions for the 2-D Linear Anisotropic–Viscoelastic Wave Equation

José M. Carcione*
Osservatorio Geofisico Sperimentale, P.O. Box 2011, 34016 Trieste, Italy, and Geophysical Institute, Hamburg University, Bundesstrasse 55, 2000 Hamburg 13, Germany

Received 23 May 1991; revised manuscript received 22 November 1993

Wave propagation simulation requires a correct implementation of boundary conditions to avoid numerical instabilities. A boundary treatment based on characteristics, which includes as special cases more simple rheologies involving isotropy and elastic behavior, is applied to the anisotropic–viscoelastic wave equation. The method introduces the boundary conditions by specifying the values of the incoming variables, which depend on the solution outside the model volume. The formulation ends up with a wave equation for the boundaries that implicitly includes the boundary conditions. The examples illustrate common problems in geophysical modeling, including free surface and nonreflecting conditions. © 1994 John Wiley & Sons, Inc.

I. INTRODUCTION

Wave propagation simulation is determined by the governing differential equations, the initial conditions, and the time-dependent boundary conditions. In addition, when solving with grid methods, nonreflecting conditions need to be implemented in order to avoid nonphysical reflections from the boundaries of the numerical mesh.

In numerical modeling, direct implementation of the boundary conditions may produce unstable schemes. The motivation of this work is to introduce, in a correct way, different types of time-dependent boundary conditions for the solution of wave propagation in linear anisotropic–viscoelastic media. Free surface, rigid, and nonreflecting boundary conditions, and, in general, any arbitrary time-dependent boundary condition are treated.

The method used here was recently developed by Thompson [1, 2]. The wave equation, recast as a first-order hyperbolic system, is decomposed into wave modes, which describe outgoing and incoming waves at the boundaries. The outgoing waves are determined by the solution within the computational volume, while the incoming waves depend on the boundary conditions. The result of this approach is a wave equation at the boundaries that automatically includes the boundary conditions. This makes the technique suitable for implicit time advancing schemes.

The next section introduces the 2-D wave equation in linear anisotropic–viscoelastic media. Section III, briefly outlines Thompson's technique. Then, Section IV applies the

Numerical Methods for Partial Differential Equations, 10, 771–791 (1994)

CCC 0749-159X/94/060771-21

method to the general anisotropic case, with special emphasis on transverse isotropy which includes the isotropic case. Section V describes several common boundary conditions in wave propagation, giving a detailed formulation for the free surface condition when the medium is transversely isotropic with symmetry axis normal to the free surface. Finally, Section VI illustrates the complete modeling scheme for a typical geophysical problem.

II. WAVE EQUATION

The wave equation for 2-D linear anisotropic and viscoelastic media, based on a particular class of constitutive laws, involves the following equations [3].

(i) The equations of momentum conservation:

$$\dot{v}_x = \frac{1}{\rho}\left(\frac{\partial \sigma_{xx}}{\partial x} + \frac{\partial \sigma_{xz}}{\partial z}\right) + f_x\,, \tag{1a}$$

$$\dot{v}_z = \frac{1}{\rho}\left(\frac{\partial \sigma_{xz}}{\partial x} + \frac{\partial \sigma_{zz}}{\partial z}\right) + f_z\,, \tag{1b}$$

where $\mathbf{x} = (x, z)$ are Cartesian coordinates, $\sigma_{xx}(\mathbf{x}, t)$, $\sigma_{xz}(\mathbf{x}, t)$, and $\sigma_{zz}(\mathbf{x}, t)$ are the stress components, $v_x(\mathbf{x}, t)$ and $v_z(\mathbf{x}, t)$ are the particle velocities, $\rho(\mathbf{x})$ denotes the density, and $f(\mathbf{x}, t) = (f_x, f_z)$ are the body forces. In (1a)–(1b) and elsewhere, time differentiation is indicated with the dot convention.

(ii) The constitutive equations:

$$\dot{\sigma}_{xx} = \hat{c}_{11}\frac{\partial v_x}{\partial x} + \hat{c}_{13}\frac{\partial v_z}{\partial z} + c_{15}\left(\frac{\partial v_x}{\partial z} + \frac{\partial v_z}{\partial x}\right) + (D - c_{55})\sum_{l=1}^{L_1}\epsilon_{1l} + c_{55}\sum_{l=1}^{L_2}\epsilon_{2l}\,, \tag{2a}$$

$$\dot{\sigma}_{zz} = \hat{c}_{13}\frac{\partial v_x}{\partial x} + \hat{c}_{33}\frac{\partial v_z}{\partial z} + c_{35}\left(\frac{\partial v_x}{\partial z} + \frac{\partial v_z}{\partial x}\right) + (D - c_{55})\sum_{l=1}^{L_1}\epsilon_{1l} - c_{55}\sum_{l=1}^{L_2}\epsilon_{2l}\,, \tag{2b}$$

$$\dot{\sigma}_{xz} = c_{15}\frac{\partial v_x}{\partial x} + c_{35}\frac{\partial v_z}{\partial z} + \hat{c}_{55}\left(\frac{\partial v_x}{\partial z} + \frac{\partial v_z}{\partial x}\right) + c_{55}\sum_{l=1}^{L_2}\epsilon_{3l}\,, \tag{2c}$$

where

$$\begin{aligned}
\hat{c}_{11} &= c_{11} - D + (D - c_{55})M_{u1} + c_{55}M_{u2}\,,\\
\hat{c}_{13} &= c_{13} + 2c_{55} - D + (D - c_{55})M_{u1} - c_{55}M_{u2}\,,\\
\hat{c}_{33} &= c_{33} - D + (D - c_{55})M_{u1} + c_{55}M_{u2}\,,\\
\hat{c}_{55} &= c_{55}M_{u2}\,,
\end{aligned}$$

are the high-frequency limit elasticities, with

$$\begin{bmatrix} c_{11} & c_{13} & c_{15} \\ & c_{33} & c_{35} \\ & & c_{55} \end{bmatrix}(\mathbf{x}) \tag{3}$$

the symmetric 2-D low-frequency limit elasticity matrix, and $D = (c_{11} + c_{33})/2$. The quantities $\epsilon_{1l}(\mathbf{x}, t)$ are memory variables related to the L_1 mechanisms, which describe the

anelastic characteristics of the quasi-dilatational mode, and $\epsilon_{2l}(\mathbf{x},t)$, $\epsilon_{3l}(\mathbf{x},t)$ are memory variables related to the L_2 mechanisms for the quasi-shear mode. $M_{uv}, v = 1,2$ are the relaxation functions evaluated at $t = 0$, with $v = 1$, the quasi-dilatational, and $v = 2$, the quasi-shear. For a general standard linear solid relaxation function, they are given by

$$M_{uv} = 1 - \sum_{l=1}^{L_v} \left(1 - \frac{\tau_{\epsilon l}^{(v)}}{\tau_{\sigma l}^{(v)}} \right), \qquad v = 1,2, \tag{4}$$

with $\tau_{\sigma l}^{(v)}$ and $\tau_{\epsilon l}^{(v)}$ the material relaxation times.

In the anisotropic-elastic limit, i.e., when $\tau_{\epsilon l}^{(v)} \to \tau_{\sigma l}^{(v)}$, and the memory variables vanish, Eqs. (2a)–(2c) become Hooke's law [4]. In the isotropic–viscoelastic limit, $c_{11}, c_{33} \to \lambda + 2\mu$, $c_{13} \to \lambda$, $c_{55} \to \mu$ and $c_{15}, c_{35} \to 0$, with λ and μ the Lame constants, and (2a)–(2c) become the isotropic–viscoelastic rheology introduced in [5]. Note that the mean stress $(\sigma_{xx} + \sigma_{zz})/2$ depends only on the parameters and memory variables with index $v = 1$, which involve quasi-dilatational dissipation mechanisms. Similarly, the deviatoric stress components, $(\sigma_{xx} - \sigma_{zz})/2$ and σ_{xz}, depend on the parameters and memory variables with index $v = 2$, involving quasi-shear mechanisms.

(iii) The memory variable equations:

$$\dot{\epsilon}_{1l} = \phi_{1l}\left(\frac{\partial v_x}{\partial x} + \frac{\partial v_z}{\partial z} \right) - \frac{\epsilon_{1l}}{\tau_{\sigma l}^{(1)}}, \qquad l = 1, \ldots, L_1, \tag{5a}$$

$$\dot{\epsilon}_{2l} = \phi_{2l}\left(\frac{\partial v_x}{\partial x} - \frac{\partial v_z}{\partial z} \right) - \frac{\epsilon_{2l}}{\tau_{\sigma l}^{(2)}}, \qquad l = 1, \ldots, L_2, \tag{5b}$$

$$\dot{\epsilon}_{3l} = \phi_{2l}\left(\frac{\partial v_x}{\partial z} + \frac{\partial v_z}{\partial x} \right) - \frac{\epsilon_{3l}}{\tau_{\sigma l}^{(2)}}, \qquad l = 1, \ldots, L_2, \tag{5c}$$

where

$$\phi_{vl} = \frac{1}{\tau_{\sigma l}^{(v)}} \left(1 - \frac{\tau_{\epsilon l}^{(v)}}{\tau_{\sigma l}^{(v)}} \right), \qquad v = 1,2. \tag{6}$$

The equations given in (i), ii), and iii) are the basis for the numerical solution algorithm. The formulation requires recasting the equations governing wave propagation as

$$-\frac{\partial \mathbf{v}}{\partial t} + \mathbf{A}\frac{\partial \mathbf{v}}{\partial x} + \mathbf{B}\frac{\partial \mathbf{v}}{\partial z} + \mathbf{d} = 0, \tag{7}$$

where

$$\mathbf{v} = \begin{bmatrix} v_x \\ v_z \\ \sigma_{xx} \\ \sigma_{zz} \\ \sigma_{xz} \\ \langle \epsilon_{1l} \rangle_{L_1} \\ \langle \epsilon_{2l} \rangle_{L_2} \\ \langle \epsilon_{3l} \rangle_{L_2} \end{bmatrix} \qquad \mathbf{d} = \begin{bmatrix} f_x \\ f_z \\ (D - c_{55}) \sum_{l=1}^{L_1} \epsilon_{1l} + c_{55} \sum_{l=1}^{L_2} \epsilon_{2l} \\ (D - c_{55}) \sum_{l=1}^{L_1} \epsilon_{1l} - c_{55} \sum_{l=1}^{L_2} \epsilon_{2l} \\ c_{55} \sum_{l=1}^{L_2} \epsilon_{3l} \\ \left\langle -\epsilon_{1l}/\tau_{\sigma l}^{(1)} \right\rangle_{L_1} \\ \left\langle -\epsilon_{2l}/\tau_{\sigma l}^{(2)} \right\rangle_{L_2} \\ \left\langle -\epsilon_{3l}/\tau_{\sigma l}^{(2)} \right\rangle_{L_2} \end{bmatrix}. \tag{8a, b}$$

and

$$\mathbf{A} = \begin{bmatrix} 0 & 0 & \rho^{-1} & 0 & 0 & 0 & \dots & 0 \\ 0 & 0 & 0 & 0 & \rho^{-1} & 0 & \dots & 0 \\ \hat{c}_{11} & c_{15} & 0 & 0 & 0 & 0 & \dots & 0 \\ \hat{c}_{13} & c_{35} & 0 & 0 & 0 & 0 & \dots & 0 \\ c_{15} & \hat{c}_{55} & 0 & 0 & 0 & 0 & \dots & 0 \\ \langle \phi_{1l} & 0 & 0 & 0 & 0 & 0 & \dots & 0 \rangle_{L_1} \\ \langle \phi_{2l} & 0 & 0 & 0 & 0 & 0 & \dots & 0 \rangle_{L_2} \\ \langle 0 & \phi_{2l} & 0 & 0 & 0 & 0 & \dots & 0 \rangle_{L_2} \end{bmatrix},$$

$$\mathbf{B} = \begin{bmatrix} 0 & 0 & 0 & 0 & \rho^{-1} & 0 & \dots & 0 \\ 0 & 0 & 0 & \rho^{-1} & 0 & 0 & \dots & 0 \\ c_{15} & \hat{c}_{13} & 0 & 0 & 0 & 0 & \dots & 0 \\ c_{35} & \hat{c}_{33} & 0 & 0 & 0 & 0 & \dots & 0 \\ \hat{c}_{55} & c_{35} & 0 & 0 & 0 & 0 & \dots & 0 \\ \langle 0 & \phi_{1l} & 0 & 0 & 0 & 0 & \dots & 0 \rangle_{L_1} \\ \langle 0 & -\phi_{2l} & 0 & 0 & 0 & 0 & \dots & 0 \rangle_{L_2} \\ \langle \phi_{2l} & 0 & 0 & 0 & 0 & 0 & \dots & 0 \rangle_{L_2} \end{bmatrix} \tag{9a, b}$$

The notation $\langle \rangle_{L_v}$ denotes a vertical a succession of elements from $l = 1, \dots, L_v$, $v = 1, 2$. The vectors have dimension $m = 5 + L_1 + 2L_2$, and matrices are of size $m \times m$. Implementation of the boundary conditions along a given direction requires the characteristic equation corresponding to (7) in that direction.

III. OUTLINE OF THE METHOD

Let the boundary be normal to the z direction. Equation (7) can be expressed as

$$-\frac{\partial \mathbf{v}}{\partial t} + \mathbf{B}\frac{\partial \mathbf{v}}{\partial z} + \mathbf{c}_z = 0, \qquad \mathbf{c}_z = \mathbf{A}\frac{\partial \mathbf{v}}{\partial x} + \mathbf{d}. \tag{10}$$

The scheme, developed by Thompson [2], determines an equation for $\partial \mathbf{v}/\partial t$ at the boundaries, where outgoing and incoming waves are decoupled. Then, the boundary conditions are introduced through the incoming waves. The method involves the following steps.

1. Compute the eigenvalues of $\mathbf{B}$ from

$$\det(\mathbf{B} - \lambda \mathrm{I}) = 0, \tag{11}$$

where I is the identity matrix. It is shown in the next section that some of the eigenvalues give the characteristic velocities of outgoing and incoming waves at the boundary.

2. Compute the left and right eigenvectors of $\mathbf{B}$, denoted by I_i and $\mathbf{r}_i$, respectively. They satisfy

$$\mathrm{I}_i^T \mathbf{B} = \lambda_i \mathrm{I}_i^T, \qquad \mathbf{B} r_i = \lambda_i \mathbf{r}_i, \qquad i = 1, \ldots, m \tag{12}$$

(since $\mathbf{B}$ is a real matrix), and the relation of mutual orthogonality,

$$\mathrm{I}_i^T \cdot \mathbf{r}_j = \delta_{ij}. \tag{13}$$

3. Construct the matrix $\mathbf{S}$ such that its columns are the right eigenvectors. The rows of the inverse $\mathbf{S}^{-1}$ are then the left eigenvectors. The diagonal matrix, whose components are the eigenvalues, are then

$$\Lambda = \mathbf{S}^{-1}\mathbf{B}\mathbf{S}. \tag{14}$$

4. Define a vector $\mathcal{H}$ by

$$\mathcal{H} \equiv \Lambda \mathbf{S}^{-1} \frac{\partial \mathbf{v}}{\partial z}, \qquad \text{or} \qquad \mathcal{H}_i \equiv \lambda_i \mathrm{I}_i^T \frac{\partial \mathbf{v}}{\partial z}, \qquad i = 1, \ldots, m. \tag{15}$$

Vector $\mathcal{H}$ includes each decoupled characteristic wave mode in the z-direction. Multiplying equation (10) from the left side by $\mathbf{S}^{-1}$, and using (15), gives

$$-\mathbf{S}^{-1}\frac{\partial \mathbf{v}}{\partial t} + \mathcal{H} + \mathbf{S}^{-1}\mathbf{c}_z = 0, \quad \text{or} \quad -\mathrm{I}_i^T \frac{\partial \mathbf{v}}{\partial t} + \mathcal{H}_i + \mathrm{I}_i^T \mathbf{c}_z = 0, \qquad i = 1, \ldots, m. \tag{16}$$

5. Multiply Eq. (16) by $\mathbf{S}$ to get the original wave equation in terms of the $\mathcal{H}_i$ variables,

$$-\frac{\partial \mathbf{v}}{\partial t} + \mathbf{S}\mathcal{H} + \mathbf{c}_z = 0. \tag{17}$$

This equation completely defines $\partial \mathbf{v}/\partial t$ at the boundaries in terms of the decoupled outgoing and incoming modes. The boundary conditions are implemented in the following way: assume that $a \le z \le b$, for points (x, a), compute $\mathcal{H}_i(\lambda_i < 0$ for outgoing waves) from Eq. (15), and $\mathcal{H}_i(\lambda_i > 0$ for incoming waves) from the boundary conditions. Similarly, for points (x, b), compute $\mathcal{H}_i(\lambda_i > 0)$ from Eq. (15), and $\mathcal{H}_i(\lambda_i < 0)$ from the boundary conditions. Then, solve Eq. (7) for the interior region, and Eq. (17) at the boundaries.

The boundaries normal to the x-direction are treated in a similar way: the equation reads

$$-\frac{\partial \mathbf{v}}{\partial t} + \mathbf{T}\mathcal{R} + \mathbf{c}_x = 0, \qquad \mathbf{c}_x = \mathbf{B}\frac{\partial \mathbf{v}}{\partial z} + \mathbf{d}, \tag{18}$$

where

$$\mathcal{R} \equiv M\mathbf{T}^{-1}\frac{\partial \mathbf{v}}{\partial x}, \qquad \text{or} \qquad \mathcal{R}_i \equiv \mu_i \mathbf{m}_i^T \frac{\partial \mathbf{v}}{\partial x}, \qquad i = 1, \ldots, m, \tag{19}$$

with M the diagonal matrix of the eigenvalues $\mu_i, i = 1, \ldots, m$. The rows of $\mathbf{T}^{-1}$ are the left eigenvectors $\mathbf{m}_i$.

At corner points, a tentative approach is to perform the characteristic analysis for both coordinates, obtaining an equation of the form

$$-\frac{\partial \mathbf{v}}{\partial t} + \mathbf{T}\mathcal{R} + \mathbf{S}\mathcal{H} + \mathbf{d} = 0. \tag{20}$$

The values of $\mathcal{R}_i$ and $\mathcal{H}_i$ are determined depending on the values of μ_i and λ_i in the x and z-directions, respectively. An alternative approach is to rotate one set of characteristics ($\mathcal{H}$ or $\mathcal{R}$) by $\pi/4$ and apply the boundary treatment.

Gottlieb, Gunzburger, and Turkel [6] developed a similar way of implementing boundary conditions in the one-dimensional elastic wave equation. For the anisotropic–viscoelastic wave equation, their approach can be interpreted as follows: define the characteristic variables vector, say the z-direction, as

$$\mathbf{W} = \mathbf{S}^{-1}\mathbf{v}, \tag{21}$$

such that Eq. (10) becomes

$$-\frac{\partial \mathbf{W}}{\partial t} + \Lambda \frac{\partial \mathbf{W}}{\partial z} + \mathbf{S}^{-1}\mathbf{c}_z = 0. \tag{22}$$

Then, Eq. (22) is the characteristic equation corresponding to (10). This approach requires that those components of $\mathbf{W}$ corresponding to outgoing characteristic variables remain unmodified after application of the boundary conditions, since these variables have their behavior entirely defined by the solution inside the physical region. Instead, those components of $\mathbf{W}$ corresponding to incoming characteristic variables are determined by the boundary conditions. In this way, the components of $\mathbf{v}$, calculated by some scheme using interior points, are corrected in order to fulfill the constraints imposed by the boundary conditions.

Applications in fluid dynamics can be found in reference [7], while references [8, 9, 10, 11] present examples in isotropic–elastic media for geophysical problems. In the same context, Canuto and Quarteroni [12] introduce a modification to this method, for application with implicit time advancing schemes. It can be shown that the method in [6], although using a different formal approach, gives identical results to Thompson's technique. However, the latter has the advantage that the eigenvectors corresponding to zero eigenvalues need not be calculated.

IV. BOUNDARY TREATMENT

Consider the problem in the z-direction: Eq. (17) has to be found in order to apply the boundary conditions. The first step involves the calculation of the eigenvalues of $\mathbf{B}$ given in Eq. (9b). They are

$$\lambda_1 = (2\rho)^{-1/2}\left(\hat{c}_{55} + \hat{c}_{33} + \sqrt{(\hat{c}_{33} - \hat{c}_{55})^2 + 4c_{35}^2}\right)^{-1/2}, \qquad \lambda_2 = -\lambda_1, \tag{23a,b}$$

$$\lambda_3 = (2\rho)^{-1/2}\left(\hat{c}_{55} + \hat{c}_{33} - \sqrt{(\hat{c}_{33} - \hat{c}_{55})^2 + 4c_{35}^2}\right)^{-1/2}, \qquad \lambda_4 = -\lambda_3, \tag{24a,b}$$

$$\lambda_i = 0, \qquad i = 5, \ldots, m. \tag{25}$$

The zero eigenvalues arise from the fact that $\mathbf{B}$ has $m - 5$ zero columns. The first four eigenvalues satisfy

$$(\rho\lambda_i^2 - \hat{c}_{55})(\rho\lambda_i^2 - \hat{c}_{33}) - c_{35}^2 = 0, \qquad i = 1,\ldots,4. \tag{26}$$

Eigenvalues λ_1 and λ_2 are the phase velocities of quasi-compressional waves moving in the positive and negative z-directions; while λ_3 and λ_4 are the corresponding velocities of the quasi-shear mode (see [3] for the expression of the phase velocities in linear anisotropic–viscoelastic media).

The next step is to find the left eigenvectors of $\mathbf{B}$ in order to construct the matrix $\mathbf{S}^{-1}$ and compute the quantities $\mathcal{H}_i$ from (15). The analysis is greatly simplified since most of the eigenvalues are zero, and only $\mathcal{H}_i, i = 1,\ldots,4$ do not vanish. To compute them, only the left eigenvectors $\mathrm{I}_i^T, i = 1,\ldots,4$ are needed. At this point, it is important to consider the case $c_{35} = c_{15} = 0$, which defines a transversely isotropic solid with symmetry axis in the z-direction, and the isotropic solid as a special case. The eigenvalues are

$$\lambda_1 = \sqrt{\hat{c}_{33}/\rho} \equiv c_P, \quad \lambda_2 = -c_P, \qquad \lambda_3 = \sqrt{\hat{c}_{55}/\rho} \equiv c_S, \quad \lambda_4 = -c_S, \quad (27a,b,c,d)$$

where the subindices P and S denote pure compressional and shear waves.

Consider first the general case with $c_{35} \neq 0$. The left eigenvector of $\mathbf{B}$ may be written as

$$\mathrm{I}_1 = \frac{1}{N}\left(\frac{p}{c_{35}}, 1, 0, \frac{1}{\rho\lambda_1}, \frac{p}{\rho c_{35}\lambda_1}, \langle 0\rangle_{L_1}, \langle 0\rangle_{L_2}, \langle 0\rangle_{L_2}\right)^T, \tag{28a}$$

$$\mathrm{I}_2 = \frac{1}{N}\left(\frac{p}{c_{35}}, 1, 0, -\frac{1}{\rho\lambda_1}, -\frac{p}{\rho c_{35}\lambda_1}, -\langle 0\rangle_{L_1}, \langle 0\rangle_{L_2}, \langle 0\rangle_{L_2}\right)^T, \tag{28b}$$

$$\mathrm{I}_3 = \frac{1}{M}\left(1, \frac{s}{c_{35}}, 0, \frac{s}{\rho c_{35}\lambda_3}, \frac{1}{\rho\lambda_3}, \langle 0\rangle_{L_1}, \langle 0\rangle_{L_2}, \langle 0\rangle_{L_2}\right)^T, \tag{28c}$$

$$\mathrm{I}_4 = \frac{1}{M}\left(1, \frac{s}{c_{35}}, 0, -\frac{s}{\rho c_{35}\lambda_3}, -\frac{1}{\rho\lambda_3}, \langle 0\rangle_{L_1}, \langle 0\rangle_{L_2}, \langle 0\rangle_{L_2}\right)^T, \tag{28d}$$

where

$$p = \rho\lambda_1^2 - \hat{c}_{33}, \qquad s = \rho\lambda_3^2 - \hat{c}_{55},$$

and the normalization factors are

$$N^2 = 2\left(1 + \frac{\rho\lambda_1^2 - \hat{c}_{33}}{\rho\lambda_1^2 - \hat{c}_{55}}\right), \qquad M^2 = 2\left(1 + \frac{\rho\lambda_3^2 - \hat{c}_{55}}{\rho\lambda_3^2 - \hat{c}_{33}}\right). \tag{30a, b}$$

The calculation of $\mathbf{S}\mathcal{H}$ in (17) requires only the first four right eigenvectors since $\mathcal{H}_i = 0, i = 5,\ldots,m$. The corresponding right eigenvectors are

$$\mathbf{r}_1 = \frac{1}{N}\left[\frac{p}{c_{35}}, 1, \frac{1}{\lambda_1}\left(\hat{c}_{13} + p\frac{c_{15}}{c_{35}}\right), \rho\lambda_1, \frac{\rho p\lambda_1}{c_{35}}, \left\langle\frac{\phi_{1l}}{\lambda_1}\right\rangle_{L_1}, \left\langle -\frac{\phi_{2l}}{\lambda_1}\right\rangle_{L_2}, \left\langle\frac{p\,\phi_{2l}}{c_{35}\lambda_1}\right\rangle_{L_2}\right]^T, \tag{31a}$$

$$\mathbf{r}_2 = \frac{1}{N}\Big[\frac{p}{c_{35}}, 1, -\frac{1}{\lambda_1}\Big(\hat{c}_{13} + p\frac{c_{15}}{c_{35}}\Big), -\rho\lambda_1, -\frac{\rho p\lambda_1}{c_{35}}, \times \Big\langle -\frac{\phi_{1l}}{\lambda_1}\Big\rangle_{L_1}, \Big\langle -\frac{\phi_{2l}}{\lambda_1}\Big\rangle_{L_2}, \Big\langle -\frac{p\phi_{2l}}{c_{35}\lambda_1}\Big\rangle_{L_2}\Big]^T, \tag{31b}$$

$$\mathbf{r}_3 = \frac{1}{M}\Big[1, \frac{s}{c_{35}}, \frac{1}{\lambda_3}\Big(c_{15} + p\frac{\hat{c}_{13}}{c_{35}}\Big), \frac{\rho s\lambda_3}{c_{35}}, \rho\lambda_3, \Big\langle \frac{s\,\phi_{1l}}{c_{35}\lambda_3}\Big\rangle_{L_1}, \Big\langle -\frac{s\phi_{2l}}{c_{35}\lambda_3}\Big\rangle_{L_2}, \Big\langle \frac{\phi_{2l}}{\lambda_3}\Big\rangle_{L_2}\Big]^T, \tag{31c}$$

$$\mathbf{r}_4 = \frac{1}{M}\Big[1, \frac{s}{c_{35}}, -\frac{1}{\lambda_3}\Big(c_{15} + p\frac{\hat{c}_{13}}{c_{35}}\Big), -\frac{\rho s\lambda_3}{c_{35}}, -\rho\lambda_3, \Big\langle -\frac{s\phi_{1l}}{c_{35}\lambda_3}\Big\rangle_{L_1}, \Big\langle \frac{s\phi_{2l}}{c_{35}\lambda_3}\Big\rangle_{L_2}, \Big\langle \frac{-\phi_{2l}}{\lambda_3}\Big\rangle_{L_2}\Big]^T, \tag{31d}$$

Next compute the quantities $\mathcal{H}_i, i = 1,\ldots,4$ from Eq. (15), giving

$$\mathcal{H}_1 = \frac{\lambda_1}{N}\Big(\frac{p\,\partial v_x}{c_{35}\partial z} + \frac{\partial v_z}{\partial z} + \frac{1}{\rho\lambda_1}\frac{\partial\sigma_{zz}}{\partial z} + \frac{p}{\rho c_{35}\lambda_1}\frac{\partial\sigma_{xz}}{\partial z}\Big), \tag{32a}$$

$$\mathcal{H}_2 = -\frac{\lambda_1}{N}\Big(\frac{p\,\partial v_x}{c_{35}\partial z} + \frac{\partial v_z}{\partial z} - \frac{1}{\rho\lambda_1}\frac{\partial\sigma_{zz}}{\partial z} - \frac{p}{\rho c_{35}\lambda_1}\frac{\partial\sigma_{xz}}{\partial z}\Big), \tag{32b}$$

$$\mathcal{H}_3 = \frac{\lambda_3}{M}\Big(\frac{\partial v_x}{\partial z} + \frac{s\,\partial v_z}{c_{35}\partial z} + \frac{s}{\rho c_{35}\lambda_3}\frac{\partial\sigma_{zz}}{\partial z} + \frac{1}{\rho\lambda_3}\frac{\partial\sigma_{xz}}{\partial z}\Big), \tag{32c}$$

$$\mathcal{H}_4 = -\frac{\lambda_3}{M}\Big(\frac{\partial v_x}{\partial z} + \frac{s\,\partial v_z}{c_{35}\partial z} - \frac{s}{\rho c_{35}\lambda_3}\frac{\partial\sigma_{zz}}{\partial z} - \frac{1}{\rho\lambda_3}\frac{\partial\sigma_{xz}}{\partial z}\Big). \tag{32d}$$

The product $\mathbf{S}\mathcal{H}$ that is required in Eq. (17) is

$$\mathbf{S}\mathcal{H} = \begin{bmatrix} \frac{1}{Nc_{35}}(\mathcal{H}_1 + \mathcal{H}_2) + \frac{1}{M}(\mathcal{H}_3 + \mathcal{H}_4) \\ \frac{1}{N}(\mathcal{H}_1 + \mathcal{H}_2) + \frac{1}{Mc_{35}}(\mathcal{H}_3 + \mathcal{H}_4) \\ \frac{1}{N\lambda_1}\Big(\hat{c}_{13} + p\frac{c_{15}}{c_{35}}\Big)(\mathcal{H}_1 - \mathcal{H}_2) + \frac{1}{M\lambda_3}\Big(c_{15} + p\frac{\hat{c}_{13}}{c_{35}}\Big)(\mathcal{H}_3 - \mathcal{H}_4) \\ \frac{\rho\lambda_1}{N}(\mathcal{H}_1 - \mathcal{H}_2) + \frac{\rho\lambda_3 s}{Mc_{35}}(\mathcal{H}_3 - \mathcal{H}_4) \\ \frac{\rho\lambda_1 p}{Nc_{35}}(\mathcal{H}_1 - \mathcal{H}_2) + \frac{\rho\lambda_3}{M}(\mathcal{H}_3 - \mathcal{H}_4) \\ \Big\langle \frac{1\phi_{1l}}{N\lambda_1}(\mathcal{H}_1 - \mathcal{H}_2) + \frac{1}{Mc_{35}\lambda_3}(\mathcal{H}_3 - \mathcal{H}_4)\Big\rangle_{L_1} \\ \Big\langle \frac{1\phi_{2l}}{N\lambda_1}(\mathcal{H}_2 - \mathcal{H}_1) + \frac{1}{Mc_{35}\lambda_3}(\mathcal{H}_4 - \mathcal{H}_3)\Big\rangle_{L_2} \\ \Big\langle \frac{1}{Nc_{35}\lambda_1}(\mathcal{H}_1 - \mathcal{H}_2) + \frac{1\phi_{2l}}{M\lambda_3}(\mathcal{H}_3 - \mathcal{H}_4)\Big\rangle_{L_2} \end{bmatrix} \tag{33}$$

Substitution of (33) into Eq. (17) completes the scheme.

Consider now a transversely isotropic solid whose symmetry axis coincides with the z-direction, thus having $c_{35} = c_{15} = 0$. In this case the left eigenvectors are

$$\mathrm{I}_1 = \frac{1}{\sqrt{2}}\left(0, 1, 0, \frac{1}{\rho c_P}, 0, \langle 0\rangle_{L_1}, \langle 0\rangle_{L_2}, \langle 0\rangle_{L_2}\right)^T, \tag{34a}$$

$$\mathrm{I}_2 = \frac{1}{\sqrt{2}}\left(0, 1, 0, -\frac{1}{\rho c_P}, 0, \langle 0\rangle_{L_1}, \langle 0\rangle_{L_2}, \langle 0\rangle_{L_2}\right)^T, \tag{34b}$$

$$\mathrm{I}_3 = \frac{1}{\sqrt{2}}\left(1, 0, 0, 0, \frac{1}{\rho c_S}, \langle 0\rangle_{L_1}, \langle 0\rangle_{L_2}, \langle 0\rangle_{L_2}\right)^T, \tag{34c}$$

$$\mathrm{I}_4 = \frac{1}{\sqrt{2}}\left(1, 0, 0, 0, -\frac{1}{\rho c_S}, \langle 0\rangle_{L_1}, \langle 0\rangle_{L_2}, \langle 0\rangle_{L_2}\right)^T, \tag{34d}$$

and the right eigenvalues are

$$\mathbf{r}_1 = \frac{1}{\sqrt{2}}\left(0, 1, \frac{\hat{c}_{13}}{c_P}, \rho c_P, 0, \left\langle \frac{\phi_{1l}}{c_P}\right\rangle_{L_1}, \left\langle -\frac{\phi_{2l}}{c_P}\right\rangle_{L_2}, \langle 0\rangle_{L_2}\right)^T, \tag{35a}$$

$$\mathbf{r}_2 = \frac{1}{\sqrt{2}}\left(0, 1, -\frac{\hat{c}_{13}}{c_P}, \rho c_P, 0, \left\langle -\frac{\phi_{1l}}{c_P}\right\rangle_{L_1}, \left\langle \frac{\phi_{2l}}{c_P}\right\rangle_{L_2}, \langle 0\rangle_{L_2}\right)^T, \tag{35b}$$

$$\mathbf{r}_3 = \frac{1}{\sqrt{2}}\left(1, 0, 0, 0, \rho c_S, \langle 0\rangle_{L_1}, \langle 0\rangle_{L_2}, \left\langle \frac{\phi_{2l}}{c_S}\right\rangle_{L_2}\right)^T, \tag{35c}$$

$$\mathbf{r}_4 = \frac{1}{\sqrt{2}}\left(1, 0, 0, 0, -\rho c_S, \langle 0\rangle_{L_1}, \langle 0\rangle_{L_2}, \left\langle -\frac{\phi_{2l}}{c_S}\right\rangle_{L_2}\right)^T, \tag{35d}$$

and the quantities $\mathcal{H}_i$ are

$$\mathcal{H}_1 = \frac{c_P}{\sqrt{2}}\left(\frac{\partial v_z}{\partial z} + \frac{1}{\rho c_P}\frac{\partial \sigma_{zz}}{\partial z}\right), \tag{36a}$$

$$\mathcal{H}_2 = -\frac{c_P}{\sqrt{2}}\left(\frac{\partial v_z}{\partial z} - \frac{1}{\rho c_P}\frac{\partial \sigma_{zz}}{\partial z}\right), \tag{36b}$$

$$\mathcal{H}_3 = \frac{c_S}{\sqrt{2}}\left(\frac{\partial v_x}{\partial z} + \frac{1}{\rho c_S}\frac{\partial \sigma_{xz}}{\partial z}\right), \tag{36c}$$

$$\mathcal{H}_4 = -\frac{c_S}{\sqrt{2}}\left(\frac{\partial v_x}{\partial z} - \frac{1}{\rho c_S}\frac{\partial \sigma_{xz}}{\partial z}\right), \tag{36d}$$

Finally, the product $\mathbf{S}\mathcal{H}$ is

$$\mathbf{S}\mathcal{H} = \begin{bmatrix} \frac{1}{\sqrt{2}}(\mathcal{H}_3 + \mathcal{H}_4) \\ \frac{1}{\sqrt{2}}(\mathcal{H}_1 + \mathcal{H}_2) \\ \frac{1}{\sqrt{2}}\frac{\hat{c}_{13}}{c_P}(\mathcal{H}_1 - \mathcal{H}_2) \\ \frac{1}{\sqrt{2}}\rho c_P(\mathcal{H}_1 - \mathcal{H}_2) \\ \frac{1}{\sqrt{2}}\rho c_S(\mathcal{H}_3 - \mathcal{H}_4) \\ \left\langle \frac{1}{\sqrt{2}}\frac{\phi_{1l}}{c_P}(\mathcal{H}_1 - \mathcal{H}_2) \right\rangle_{L_1} \\ \left\langle \frac{1}{\sqrt{2}}\frac{\phi_{2l}}{c_P}(\mathcal{H}_2 - \mathcal{H}_1) \right\rangle_{L_2} \\ \left\langle \frac{1}{\sqrt{2}}\frac{\phi_{2l}}{c_S}(\mathcal{H}_3 - \mathcal{H}_4) \right\rangle_{L_2} \end{bmatrix}. \tag{37}$$

Substitution of (37) into Eq. (17) gives the wave propagation equations in terms of the decoupled outgoing and incoming modes,

$$\dot{v}_x = \frac{1}{\rho}\frac{\partial \sigma_{xx}}{\partial x} + \frac{1}{\sqrt{2}}(\mathcal{H}_3 + \mathcal{H}_4) + f_x, \tag{38a}$$

$$\dot{v}_z = \frac{1}{\rho}\frac{\partial \sigma_{xz}}{\partial x} + \frac{1}{\sqrt{2}}(\mathcal{H}_1 + \mathcal{H}_2) + f_z, \tag{38b}$$

$$\dot{\sigma}_{xx} = \hat{c}_{11}\frac{\partial v_x}{\partial x} + \frac{1}{\sqrt{2}}\frac{\hat{c}_{13}}{c_P}(\mathcal{H}_1 - \mathcal{H}_2) + (D - c_{55})\sum_{l=1}^{L_1}\epsilon_{1l} + c_{55}\sum_{l=1}^{L_2}\epsilon_{2l}, \tag{38c}$$

$$\dot{\sigma}_{zz} = \hat{c}_{13}\frac{\partial v_x}{\partial x} + \frac{1}{\sqrt{2}}\rho c_P(\mathcal{H}_1 - \mathcal{H}_2) + (D - c_{55})\sum_{l=1}^{L_1}\epsilon_{1l} - c_{55}\sum_{l=1}^{L_2}\epsilon_{2l}, \tag{38d}$$

$$\dot{\sigma}_{xz} = \hat{c}_{55}\frac{\partial v_z}{\partial x} + \frac{1}{\sqrt{2}}\rho c_S(\mathcal{H}_3 - \mathcal{H}_4) + c_{55}\sum_{l=1}^{L_2}\epsilon_{3l}, \tag{38e}$$

$$\dot{\epsilon}_{1l} = \phi_{1l}\left[\frac{\partial v_x}{\partial x} + \frac{1}{\sqrt{2}\,c_P}(\mathcal{H}_1 - \mathcal{H}_2)\right] - \frac{\epsilon_{1l}}{\tau_{\sigma l}^{(1)}}, \qquad l = 1, \ldots, L_1, \tag{38f}$$

$$\dot{\epsilon}_{2l} = \phi_{2l}\left[\frac{\partial v_x}{\partial x} + \frac{1}{\sqrt{2}\,c_P}(\mathcal{H}_2 - \mathcal{H}_1)\right] - \frac{\epsilon_{2l}}{\tau_{\sigma l}^{(2)}}, \qquad l = 1, \ldots, L_2, \tag{38g}$$

$$\dot{\epsilon}_{3l} = \phi_{2l}\left[\frac{\partial v_z}{\partial x} + \frac{1}{\sqrt{2}\,c_S}(\mathcal{H}_3 - \mathcal{H}_4)\right] - \frac{\epsilon_{3l}}{\tau_{\sigma l}^{(2)}}, \qquad l = 1, \ldots, L_2. \tag{38h}$$

The equations describing wave propagation are evaluated in the form of (17) at the z boundaries, where the quantities $\mathcal{H}_i$, representing incoming variables, depend on the boundary conditions.

One important result obtained from the boundary treatment is that the quantities $\mathcal{H}$ depend only on the unrelaxed elasticities, i.e., the characteristics are not affected by the memory effects, since they depend only on the instantaneous response of the medium. This is in agreement with the results obtained by Herrera and Gurtin [13], who found that the discontinuity surface of the wavefront in a dissipative medium travels with a velocity related to the unrelaxed part of the relaxation tensor.

V. BOUNDARY CONDITIONS

For simplicity, the transversely isotropic solid is considered. The method requires that for the interior points $a < z < b$, Eq. (7) must be solved, while for $z = a$ and $z = b$, Eq. (17) or (38a)–(38h) are used. Those variables $\mathcal{H}_i$ that represent outgoing characteristics are calculated from their definitions in (36a)–(36d) while those that represent incoming characteristics are specified from the boundary conditions. An explicit derivation of Eq. (17) is performed here for the free surface boundary conditions to illustrate the technique in detail. The treatment is also outlined for nonreflecting, Dirichlet and Neumann boundary conditions, and for a boundary separating two material regions.

A. Free Surface Boundary Conditions

At the surface of the earth, for instance, force-free boundary conditions hold. Consider that the surface is normal to the z-direction. This means that the normal stresses are zero at all times. Thus, the initial conditions at the surface should include $\sigma_{zz} = \sigma_{xz} = 0$, say at $z = b = 0$. The incoming waves correspond to $\lambda_2 = -c_P$ and $\lambda_4 = -c_S$. Then, $\mathcal{H}_2$ and $\mathcal{H}_4$ must be computed from the boundary conditions. From Eqs. (38d) and (38e), σ_{zz} and σ_{xz} will remain zero at the surface if

$$\mathcal{H}_2 = \mathcal{H}_1 + \frac{\sqrt{2}}{\rho c_P}\left[\hat{c}_{13}\frac{\partial v_x}{\partial x} + (D - c_{55})\sum_{l=1}^{L_1}\epsilon_{1l} - c_{55}\sum_{l=1}^{L_2}\epsilon_{2l}\right], \tag{39a}$$

$$\mathcal{H}_4 = \mathcal{H}_3 + \frac{\sqrt{2}}{\rho c_S}\left[\hat{c}_{55}\frac{\partial v_z}{\partial x} + c_{55}\sum_{l=1}^{L_2}\epsilon_{3l}\right]. \tag{39b}$$

Substituting $\mathcal{H}_1$ and $\mathcal{H}_3$ from Eqs. (32a) and (32c) into (39a) and (39b), and the results into Eqs. (38e)–(38h), yields

$$\dot{v}_x = \frac{1}{\rho}\left(\frac{\partial \sigma_{xx}}{\partial x} + \frac{\partial \sigma_{xz}}{\partial z}\right) + \frac{1}{\rho c_S}\left[\hat{c}_{55}\left(\frac{\partial v_x}{\partial z} + \frac{\partial v_z}{\partial x}\right) + c_{55}\sum_{l=1}^{L_2}\epsilon_{3l}\right] + f_x, \tag{40a}$$

$$\dot{v}_z = \frac{1}{\rho}\left(\frac{\partial \sigma_{xz}}{\partial x} + \frac{\partial \sigma_{zz}}{\partial z}\right) + \frac{1}{\rho c_P} \times \left[\hat{c}_{13}\left(\frac{\partial v_x}{\partial x} + \hat{c}_{33}\frac{\partial v_z}{\partial z}\right) + (D - c_{55})\sum_{l=1}^{L_1}\epsilon_{1l} - c_{55}\sum_{l=1}^{L_2}\epsilon_{2l}\right] + f_z, \tag{40b}$$

$$\dot{\sigma}_{xx} = \left(\hat{c}_{11} - \frac{\hat{c}_{13}^2}{\hat{c}_{33}}\right)\frac{\partial v_x}{\partial x} + \left(1 - \frac{\hat{c}_{13}}{\hat{c}_{33}}\right)(D - c_{55})\sum_{l=1}^{L_1}\epsilon_{1l} + \left(1 + \frac{\hat{c}_{13}}{\hat{c}_{33}}\right)c_{55}\sum_{l=1}^{L_2}\epsilon_{2l}\,, \tag{40c}$$

$$\dot{\sigma}_{zz} = 0\,, \tag{40d}$$

$$\dot{\sigma}_{xz} = 0\,, \tag{40e}$$

$$\dot{\epsilon}_{1l} = \phi_{1l}\left(1 - \frac{\hat{c}_{13}}{\hat{c}_{33}}\right)\frac{\partial v_x}{\partial x} - \frac{\phi_{1l}}{\hat{c}_{33}}\left[(D - c_{55})\sum_{l'=1}^{L_1}\epsilon_{1l'} - c_{55}\sum_{l'=1}^{L_2}\epsilon_{2l'}\right] - \frac{\epsilon_{1l}}{\tau_{\sigma l}^{(1)}}, \qquad l = 1,\ldots,L_1\,, \tag{40f}$$

$$\dot{\epsilon}_{2l} = \phi_{2l}\left(1 + \frac{\hat{c}_{13}}{\hat{c}_{33}}\right)\frac{\partial v_x}{\partial x} + \frac{\phi_{2l}}{\hat{c}_{33}}\left[(D - c_{55})\sum_{l'=1}^{L_1}\epsilon_{1l'} - c_{55}\sum_{l'=1}^{L_2}\epsilon_{2l'}\right] - \frac{\epsilon_{2l}}{\tau_{\sigma l}^{(2)}}, \qquad l = 1,\ldots,L_2\,, \tag{40g}$$

$$\dot{\epsilon}_{3l} = -\phi_{2l}\frac{c_{55}}{\hat{c}_{55}}\sum_{l'=1}^{L_2}\epsilon_{3l'} - \frac{\epsilon_{3l}}{\tau_{\sigma l}^{(2)}}, \qquad l = 1,\ldots,L_2\,. \tag{40h}$$

These are the equations to be used at the free surface. They further simplify to

$$\dot{v}_x^{(new)} = \dot{v}_x^{(old)} + \frac{1}{\rho c_S}\dot{\sigma}_{xz}^{(old)}\,, \tag{41a}$$

$$\dot{v}_z^{(new)} = \dot{v}_z^{(old)} + \frac{1}{\rho c_P}\dot{\sigma}_{zz}^{(old)}\,, \tag{41b}$$

$$\dot{\sigma}_{xx}^{(new)} = \dot{\sigma}_{xx}^{(old)} - \frac{\hat{c}_{13}}{\hat{c}_{33}}\dot{\sigma}_{zz}^{(old)}\,, \tag{41c}$$

$$\dot{\sigma}_{zz}^{(new)} = 0\,, \tag{41d}$$

$$\dot{\sigma}_{xz}^{(new)} = 0\,, \tag{41e}$$

$$\dot{\epsilon}_1^{(new)} = \dot{\epsilon}_1^{(old)} - \frac{\phi_1}{\hat{c}_{33}}\dot{\sigma}_{zz}^{(old)}\,, \tag{41f}$$

$$\dot{\epsilon}_2^{(new)} = \dot{\epsilon}_2^{(old)} + \frac{\phi_2}{\hat{c}_{33}}\dot{\sigma}_{zz}^{(old)}\,, \tag{41g}$$

$$\dot{\epsilon}_3^{(new)} = \dot{\epsilon}_3^{(old)} - \frac{\phi_2}{\hat{c}_{55}}\dot{\sigma}_{xz}^{(old)}\,, \tag{41h}$$

where the superscript (old) indicates the variables given by Eq. (1)–(5), and the superscript (new) refers to the variables of the left-hand side of Eq. (40b) after modification of the incoming characteristics.

B. Nonreflecting Boundary Conditions

Suppose that $z = a = -z_0$ is a nonphysical boundary of the numerical mesh. Then, the incoming wave must be suppressed to avoid reflected waves. The incoming variables are $\mathcal{H}_1$ and $\mathcal{H}_3$. The first and third components of (16) give the following characteristics equations:

$$-\frac{\partial}{\partial t}\left[\frac{1}{\sqrt{2}}\left(v_z + \frac{1}{\rho c_P}\sigma_{zz}\right)\right] + \mathcal{H}_1 + \frac{1}{\sqrt{2}}\left\{\frac{1}{\rho}\frac{\partial \sigma_{xz}}{\partial x} + \frac{1}{\rho c_P}\left[\hat{c}_{13}\frac{\partial v_x}{\partial x} + (D - c_{55})\sum_{l=1}^{L_1}\epsilon_{1l} - c_{55}\sum_{l=1}^{L_2}\epsilon_{2l}\right] + f_z\right\} = 0, \quad (42a)$$

$$-\frac{\partial}{\partial t}\left[\frac{1}{\sqrt{2}}\left(v_x + \frac{1}{\rho c_S}\sigma_{xz}\right)\right] + \mathcal{H}_3 + \frac{1}{\sqrt{2}}\left[\frac{1}{\rho}\frac{\partial \sigma_{xx}}{\partial x} + \frac{1}{\rho c_S}\left(\hat{c}_{55}\frac{\partial v_z}{\partial x} + c_{55}\sum_{l=1}^{L_2}\epsilon_{3l}\right) + f_x\right] = 0, \quad (42b)$$

with the left eigenvectors from (34a)–(34b). These equations contain the time derivatives of the amplitudes of the incoming characteristic waves. Imposing constant amplitudes in time is equivalent to suppressing the incoming waves. This can be done by choosing

$$\mathcal{H}_1 = -\frac{1}{\sqrt{2}}\left\{\frac{1}{\rho}\frac{\partial \sigma_{xz}}{\partial x} + \frac{1}{\rho c_P}\left[\hat{c}_{13}\frac{\partial v_x}{\partial x} + (D - c_{55})\sum_{l=1}^{L_1}\epsilon_{1l} - c_{55}\sum_{l=1}^{L_2}\epsilon_{2l}\right] + f_z\right\}, \quad (43a)$$

$$\mathcal{H}_3 = -\frac{1}{\sqrt{2}}\left[\frac{1}{\rho}\frac{\partial \sigma_{xx}}{\partial x} + \frac{1}{\rho c_S}\left[\hat{c}_{55}\frac{\partial v_z}{\partial x} + c_{55}\sum_{l=1}^{L_2}\epsilon_{3l}\right] + f_x\right], \quad (43b)$$

while $\mathcal{H}_2$ and $\mathcal{H}_4$ are computed from Eq. (36b) and (36d), respectively. Since the method is based on one-dimensional characteristics (perpendicular to the boundary), non-normal incident waves may not be completely eliminated.

C. Time-Dependent Boundary Conditions

For Dirichlet boundary conditions, the particle velocities may have an arbitrary variation with time. Assuming that $v_x = u(t)$ and $v_z = w(t)$ at $z = b$, with initial data $v_x(t = 0) = u(0)$ and $v_z = w(0)$, the incoming variables are chosen so that

$$\mathcal{H}_2 = -\mathcal{H}_1 + \sqrt{2}\left(\dot{w} - \frac{1}{\rho}\frac{\partial \sigma_{xz}}{\partial x} - f_z\right), \quad (44a)$$

$$\mathcal{H}_4 = -\mathcal{H}_3 + \sqrt{2}\left(\dot{u} - \frac{1}{\rho}\frac{\partial \sigma_{xx}}{\partial x} - f_x\right), \quad (44b)$$

according to Eqs. (38a) and (38b). The outgoing variables $\mathcal{H}_1$ and $\mathcal{H}_3$ are computed from Eqs. (36a) and (36b), respectively. A special case are the rigid boundary conditions, where the particle velocities are zero at all times, i.e., $u(t) = w(t) = 0$.

Another possibility is to have stress or Neumann boundary conditions, for instance, the normal stresses, $\sigma_{zz} = f(t)$ and $\sigma_{xz} = g(t)$. From Eqs. (38d) and (38e), these conditions apply if

$$\mathcal{H}_2 = \mathcal{H}_1 + \frac{\sqrt{2}}{\rho c_P}\left[\hat{c}_{13}\frac{\partial v_x}{\partial x} + (D - c_{55})\sum_{l=1}^{L_1}\epsilon_{1l} - c_{55}\sum_{l=1}^{L_2}\epsilon_{2l} - \dot{f}\right], \tag{45a}$$

$$\mathcal{H}_4 = \mathcal{H}_3 + \frac{\sqrt{2}}{\rho c_S}\left[\hat{c}_{55}\frac{\partial v_z}{\partial x} + c_{55}\sum_{l=1}^{L_2}\epsilon_{3l} - \dot{g}\right]. \tag{45b}$$

For example, in exploration geophysics, the source is practically located at the surface. A vertical source function can be introduced as a boundary condition by taking $f(t)$ as the source time history, and $g(t) = 0$.

D. Boundary Separating Two Physical Regions

This situation may occur when solving a problem by domain decomposition. Then, at the interface separating the subdomains, the appropriate boundary conditions must be implemented. The present method suggests a way to handle this problem. One can impose continuity of $\mathbf{v}$, and choose the incoming variables of one region equal to the outgoing variables of the other region, and vice versa. This approach should give similar results to the characteristic weighting proposed in [14].

A characteristic approach can be used at a physical boundary separating two regions. For instance, at the interface between a solid and a fluid, the normal particle velocity and normal stress components are continuous when crossing the interface; in a solid-solid boundary, both horizontal and vertical particle velocity components and normal stress are continuous.

VI. NUMERICAL SCHEME

A typical problem in exploration geophysics is wave propagation in the presence of free surface boundary conditions. A seismic reflection survey uses an explosion, close to the surface, and records the earth response at receivers located on the surface. The solution is discretized in time as well as in space. The modeling algorithm consists of the calculation of the spatial derivatives, incorporation of the boundary conditions, and time integration.

A. Computation of the Spatial Derivatives

Spectral methods can be used to compute the spatial derivatives in Eq. (7). For instance, in the horizontal direction, the Fourier pseudospectral method is convenient, since it is efficient in terms of the number of grid points per wavelength. However, this method is not appropriate for the vertical direction since it cannot handle the recording configuration mentioned before, with source and receivers close to the free surface. In the vertical direction, Chebychev differentiation can be used [9]. The method is nonperiodic and provides high accuracy and high resolution at the surface. When solving the problem with an explicit time marching algorithm, Chebychev methods require time steps of order

$O(N^{-2})$, where N is the number of grid points. A new algorithm, developed by Kosloff and Tal-Ezer [15], based on a coordinate transformation, allows time steps of order $O(N^{-1})$, which are those required also by the Fourier pseudospectral method.

B. Time Integration

An efficient time integration algorithm is the fourth-order Runge–Kutta method (e.g., [14]). Let the spatial derivative operations in Eq. (7) be abbreviated to

$$\mathbf{M} = \mathbf{A}\frac{\partial}{\partial x} + \mathbf{B}\frac{\partial}{\partial z}. \tag{46}$$

If dt is the time step, the solution $\mathbf{v}^{n+1}$ at time $(n+1)\,dt$ is obtained in terms of the solution $\mathbf{v}^n$ at time ndt as

$$\mathbf{v}^{n+1} = \mathbf{v}^n - \frac{1}{6}\,dt(\Delta_1 + 2\Delta_2 + 2\Delta_3 + \Delta_4), \tag{47a}$$

where

$$\Delta_1 = \mathbf{M}\mathbf{v}^n + \mathbf{d}^n, \tag{47b}$$

$$\Delta_2 = \mathbf{M}\left(\mathbf{v}^n + \frac{dt}{2}\Delta_1\right) + \mathbf{d}^{n+\frac{1}{2}}, \tag{47c}$$

$$\Delta_3 = \mathbf{M}\left(\mathbf{v}^n + \frac{dt}{2}\Delta_2\right) + \mathbf{d}^{n+\frac{1}{2}}, \tag{47d}$$

$$\Delta_4 = \mathbf{M}(\mathbf{v}^n + dt\Delta_3) + \mathbf{d}^{n+1}. \tag{47e}$$

As mentioned before, a favorable stability condition is achieved with $dt = O(N^{-1})$.

C. Boundary Conditions

At the free surface, the boundary conditions are applied as in Section V, whereas for the bottom boundary, nonreflecting conditions are implemented. Since for nonvertical incidence, the incoming waves may not be eliminated completely, an absorbing strip is added to improve efficiency [16]. Similar absorbing regions are placed along the boundaries in the horizontal direction to avoid wraparound caused by the periodic properties of the Fourier method. The boundary conditions are automatically implemented when solving Eqs. (47a)–(47e) with the appropriate operator $\mathbf{M}$ obtained from Eq. (17) or (38a)–(38e).

D. Results

Firstly, the nonreflecting condition is tested at an upper boundary. In this example, the medium is elastic with compressional and shear wave velocities of 3000 m/s and 2000 m/s, respectively. The source has a central frequency of 25 Hz, and it is located at 200 m from the upper boundary. The effectiveness of the boundary conditions, and nonreflecting boundary conditions, respectively. As can be seen in Fig. 1(b), the reflected body waves (incoming waves) have been eliminated almost completely. Residual reflections can be eliminated by including absorbing strips.

The second example simulates a seismic reflection survey over a homogeneous half-space (actually, it is equivalent to Lamb's problem). The low-frequency limit compressional and shear wave velocities are taken as $V_P = 2000$ m/s and $V_S = 1155$ m/s,

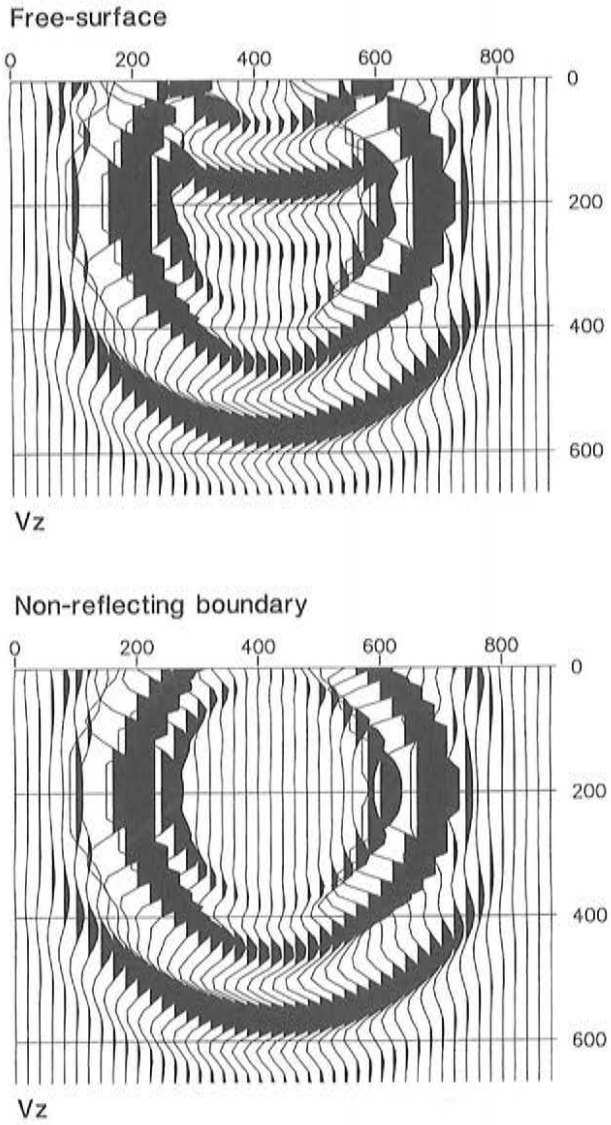

FIG. 1. Comparison between vertical component snapshots at $t = 0.18$ s propagating time: (a) free surface boundary condition and (b) nonreflecting boundary condition.

respectively, corresponding to a Poisson solid; the density is $\rho = 1$ kg/m^3. Two sets of relaxation times are used, such that the quality factors are nearly constant over the exploration seismic band. The quality factors for P and S waves turn out to be $Q_P = 30$, $Q_S = 20$, respectively.

The computation uses a grid size of $N_x = 135$ and $N_z = 81$, with uniform grid spacing $DX = 20$ m in the horizontal direction, and a largest vertical grid spacing of $DZ = 20$ m. A vertical point force is applied at grid point 20 at a depth of 1.8 m. The source is a shifted zero-phase Ricker wavelet with a central frequency of

11 Hz, and high-cutoff frequency of 22 Hz. The P and S phase velocities are 2052 m/s and 1200 m/s, respectively, at the central frequency of the source. These values indicate that significant dispersion is expected, with the anelastic wavefields traveling faster than the low-frequency elastic wavefields. The numerical solution is propagated to 2 s with a time step of 1 ms.

The seismic response is recorded at the same dept as the source position. Figure 2 compares elastic and anelastic seismograms with (a) horizontal components, and (b) vertical components. As can be appreciated, the compressional wave loses amplitude with time due to geometrical spreading, while the Rayleigh wave keeps the same amplitude

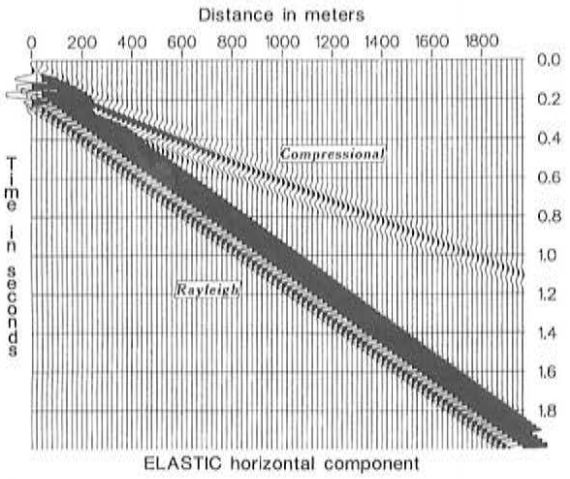

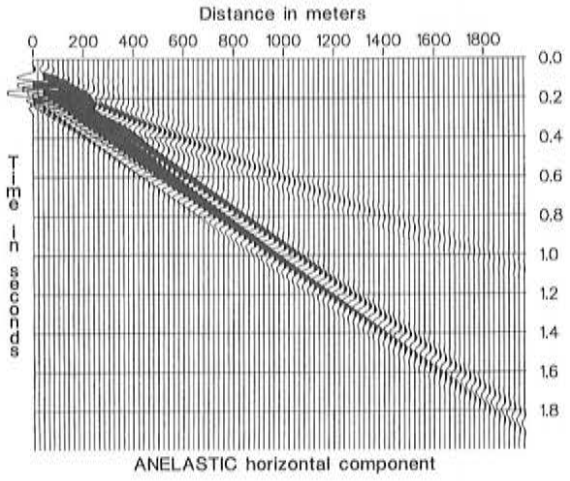

(a)

FIG. 2. Comparison between elastic and anelastic seismograms recorded at the surface of the earth: (a) horizontal components and (b; next page) vertical components.

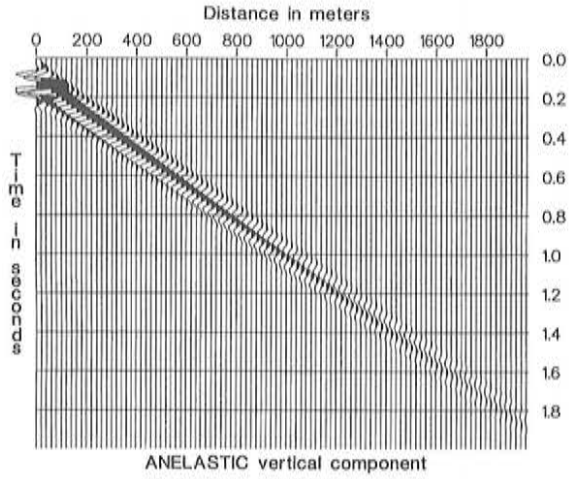

(b)

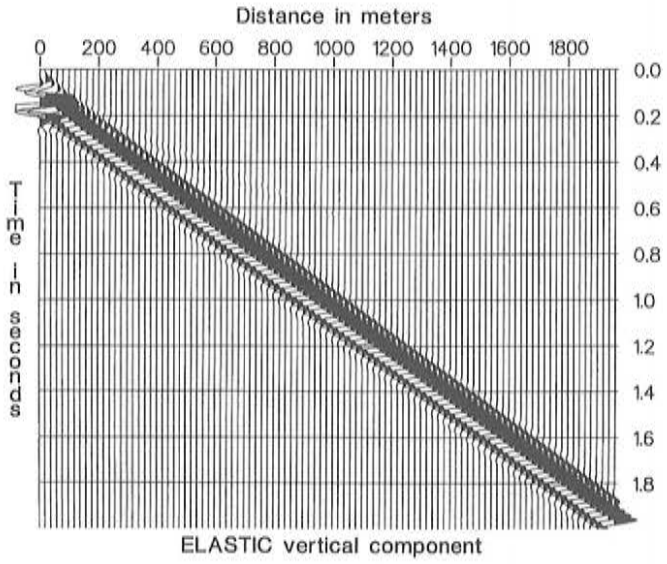

FIG. 2. (Continued)

since it is confined to the surface. On the contrary, in the anelastic medium, the atenuation and velocity dispersion affect the surface wave considerably. Note that the seismogram is free from reflected events coming from the bottom, where a nonreflecting boundary condition and absorbing strip have been implemented. The performance of the method is better illustrated in Fig. 3, which compares elastic (a) and anelastic (b) snapshots of the horizontal components at 0.75 s and 1.25 s propagation times. The P and S waves hit the bottom boundary with a wide range of incidence angles, but no artificial reflected event is seen.

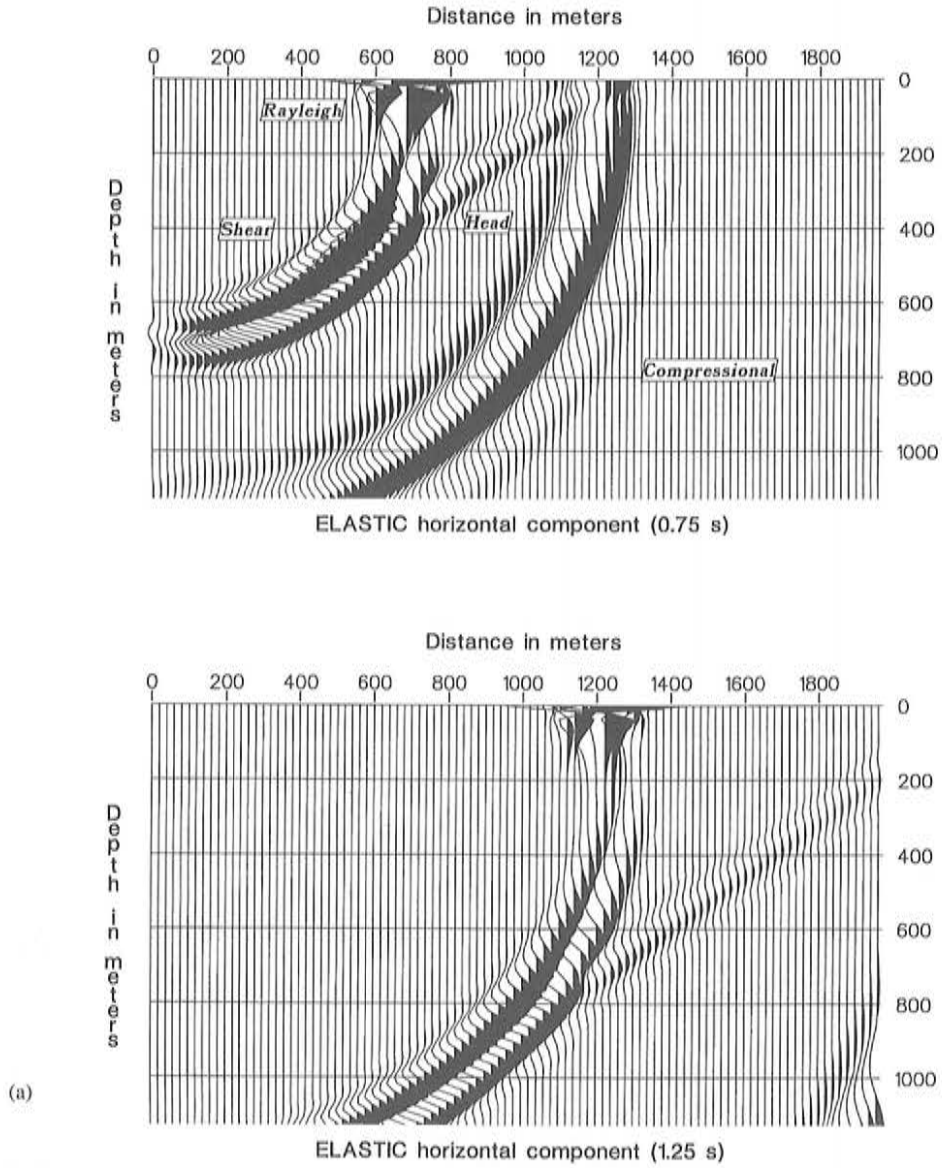

FIG. 3. Comparison between elastic and anelastic snapshots of the horizontal component at different propagation times, where (a) is elastic and (b; next page) is viscoelastic.

VII. CONCLUSIONS

Decoupling the wave equation into outgoing and incoming waves at a boundary allows a correct implementation of boundary conditions. Despite the complexity of the anisotropic–viscoelastic wave equation due to the presence of memory variables, a closed expression of the correct wave equation at the boundaries is obtained. The analysis

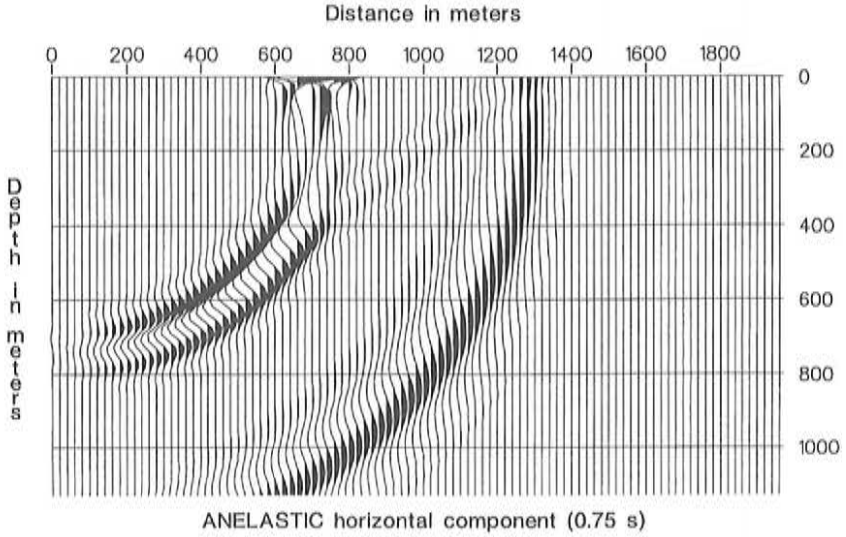

(b)

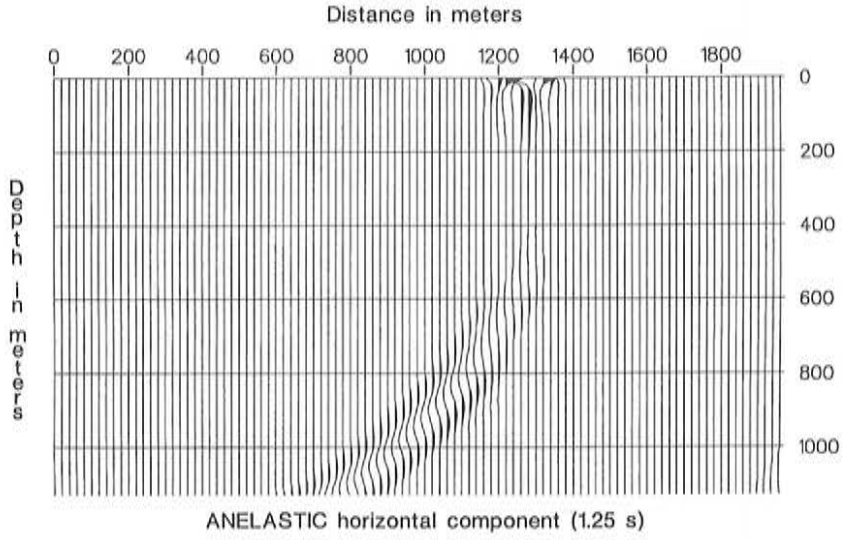

FIG. 3. (Continued)

includes the simplest case, the isotropic–elastic, and more complex rheologies up to the general anisotropic–viscoelastic case. Future work involves extension into 3-D, testing of the different boundary conditions for different rheologies, and applications to practical problems.

This work was supported in part by the Commission of the European Communities under the GEOSCIENCE project. The author wishes to thank Fabio Cavallini for his many suggestions during the course of the research.

References

1. K. W. Thompson, "Time-dependent boundary conditions for hyperbolic systems, I," *J. Comput. Phys.* **68**, 1 (1987).
2. K. W. Thompson, "Time-dependent boundary conditions for hyperbolic systems, II," *J. Comput. Phys.* **89**, 439 (1990).
3. J. M. Carcione, "Wave propagation in anisotropic linear viscoelastic media: theory and simulated wavefields," *Geophys. Int.* **101**, 739 (1990).
4. J. M. Carcione, D. Kosloff, and R. Kosloff, "Wave propagation simulation in an anisotropic (transversely isotropic) medium," *Q. Jl. Mech. Appl. Math.* **41**, 319 (1988).
5. J. M. Carcione, D. Kosloff, and R. Kosloff, "Wave propagation simulation in a linear viscoelastic medium," *Geophys. J. Roy. Astr. Soc.* **95**, 597 (1988).
6. D. Gottlieb, M. D. Gunzberger, and E. Turkel, "On numerical boundary treatment for hyperbolic systems," *SIAM J. Numer. Anal.* **19**, 671 (1982).
7. D. Gottlieb, L. Lustman, and C. Streett, "Spectral methods for two-dimensional shocks," in *Proceedings, symposium on spectral methods for partial differential equations,* R. G. Voight, et al. Eds., NASA Langley Research Center, 1982 (SIAM), p. 79.
8. A. Bayliss, K. E. Jordan, B. J. Lemesurier, and E. Turkel, "A fourth order accurate finite-difference scheme for the computation of elastic waves," *Bull. Seism. Soc. Am.* **76**, 1115–1132 (1986).
9. D. Kosloff, D. Kessler, A. Queiroz Filho, E. Tessmer, A. Behle, and R. Strahilevitz, "Solution of the equations of dynamic elasticity by a Chebychev spectral method," *Geophysics* **55**, 734 (1990).
10. D. Kessler and D. Kosloff, "Acoustic wave propagation in 2-D cylindrical coordinates," *Geophys. J. Int.* **103**, 577 (1990).
11. E. Tessmer, D. Kessler, D. Kosloff, and A. Behle, "Multi-domain Chebyshev–Fourier method for the solution of the equation of motion of dynamic elasticity," *J. Comput. Phys.* **100**, 355 (1992).
12. C. Canuto and A. Quarteroni, "On the boundary treatment in spectral methods for hyperbolic systems," *J. Comput. Phys.* **71**, 100 (1987).
13. I. Herrera and M. E. Gurtin, "A correspondence principle for viscoelastic wave propagation," *Quart. Appl. Math.* **22**, 360 (1965).
14. C. Canuto, M. Y. Hussaini, A. Quarteroni, and T. A. Zang, *Spectral Methods in Fluid Dynamics,* Springer Verlag, 1988, p. 450.
15. D. Kosloff and H. Tal-Ezer, "A modified Chebyshev pseudospectral method with an $O(N^{-1})$ time step restriction," *J. Comput. Phys.* **104**, 457 (1993).
16. R. Kosloff and D. Kosloff, "Absorbing boundaries for wave propagation problems," *J. Comput. Phys.* **63**, 363 (1986).